Polymer 150 (2018) 244–253

Contents lists available at ScienceDirect

Polymer

journal homepage: www.elsevier.com/locate/polymer

Rouse dynamics in PEO-PPO-PEO block-copolymers in aqueous solution as observed through fast field-cycling NMR relaxometry

Carla C. Fraenza [a], Carlos Mattea [b], Germán D. Farrher [a], Amín Ordikhani-Seyedlar [b], Siegfried Stapf [b, *], Esteban Anoardo [a, **]

[a] Laboratorio de Relaxometría y Técnicas Especiales, Grupo de RMN, Facultad de Matemática, Astronomía, Física y Computación, Universidad Nacional de Córdoba and IFEG-CONICET, Córdoba, Argentina
[b] Technische Universität Ilmenau, Institüt für Physik, Fachbereit Technische Physik II: Polymerphysik, Ilmenau, Germany

ARTICLE INFO

Article history:
Received 10 February 2018
Received in revised form
7 July 2018
Accepted 10 July 2018
Available online 12 July 2018

Keywords:
NMR Relaxometry
Pluronics
Polymeric vesicles

ABSTRACT

We present a proton fast field-cycling (FFC) NMR relaxometry study of the molecular dynamics in three different deuterated water-dispersed triblock copolymers of ethylene oxide (EO) and propylene oxide (PO):$EO_{80}PO_{27}EO_{80}$(F68), $EO_{141}PO_{44}EO_{141}$ (F108), and $EO_{101}PO_{56}EO_{101}$(F127). Independently of the phase and molecular arrangement, bi-exponential decays of the magnetization during the spin-lattice relaxation process could be observed for F127, while mono-exponential decays were measured for F68 and F108. This fact has been attributed to the relative ratio of PEO and PPO protons for each case. In F127, each component of the magnetization decay could be associated with a particular block of the co-polymer. A direct consequence of this fact is the independent characterization of the molecular dynamics of each block. It was found that the dominant relaxation mechanism can be attributed to the Rouse model, and it seems to be independent on whether the molecules are incorporated into a micelle, or as individual unimers in the aqueous solution. The experimental results and the provided explanation are consistent with entanglement-free self-assembled structures, and a fast exchange of unimers between the micellar structure and the solvent. This particular feature was also investigated in F68 and F108, although for these cases a mono-exponential decay of the magnetization was observed. NMR relaxometry results are complemented with other relaxation experiments in the rotating frame, NMR spectroscopy and atomic-force microscopy.

1. Introduction

The study here presented is focused on poly(ethylene oxide) - poly(propylene oxide) - poly(ethylene oxide) (PEO-PPO-PEO), commercially available from different companies, being also known in the literature by their trade names (in our case Pluronic from BASF). The system can be purchased with different molecular weights and lengths for the PEO/PPO chains. In this work we measure the ^1H spin-lattice relaxation dispersion of the amphiphilic specimens dispersed in D_2O.

In water solution, this copolymer exhibits a noticeable temperature and concentration dependent mesomorphic behavior [1,2]. At low concentrations and temperatures, the block copolymers dissolve in water as individual entities (unimers). By increasing concentration and/or temperature, critical values trigger a micellization process [3,4] and they are called critical micellization concentration (CMC) and critical micellization temperature (CMT). The micellization behavior is also dependent on the polymer structure and its molecular weight [1]. The micelles architecture consists of a hydrophobic core (PPO) and a hydrophilic corona (PEO) with typical hydrodynamic radii of the order of 10 nm, tending to form clusters with aggregation numbers of the order of 50 units. This number is weakly dependent on the copolymer concentration, but increases with the temperature [5]. A schematic representation of the structure of unimers and micelles in an aqueous solution is shown in Fig. 1. By increasing the concentration, micelles tend to be arranged in a close-packed array until gelation occurs due to a weak entanglement (soft gel), or a strong entanglement (hard gel) among the corona PEO chains [6]. The gel phase

* Corresponding author.
** Corresponding author.
E-mail addresses: siegfried.stapf@tu-ilmenau.de (S. Stapf), anoardo@famaf.unc.edu.ar (E. Anoardo).

https://doi.org/10.1016/j.polymer.2018.07.027
0032-3861/

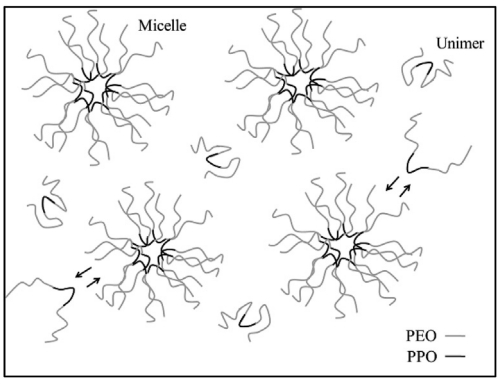

Fig. 1. Schematic representation of the structure of unimers and micelles in an aqueous solution. It shows the coexistence of them when the concentration of the triblock copolymer is larger than the critical micellization concentration (CMC). The exchange kinetics of unimers from the bulk into the micelle and vice versa is also represented by the two black arrows (see text for explanation).

can also be reached by increasing the temperature, due to a dehydration of the PEO and PPO moieties [7]. Usually unimers, micelles and micellar aggregates coexist, showing up one dominant phase according to the concentration and temperature [8].

Dynamical features of the copolymer/micelle occur over a broad timescale, covering several decades from $<10^{-12}$ s for fast molecular vibrational and rotational modes of the internal groups conforming the unimers and bulklike ultrafast dynamics [9], up to much slower motions associated to reorientations of clusters and micelle fusion-fission processes (>1 s) [10]. While many experimental techniques have been used for the study of the dynamics in these systems, most of these are only capable of monitoring a single aspect of the dynamics on a very limited timescale. Typical examples are time resolved emission spectroscopy [11], nuclear magnetic resonance (NMR) spectroscopy [12,13], NMR diffusion [14,15] and high-field relaxation [16], temperature jump [17], ultrasonic absorption [18] and neutron scattering [19]. Experimentally determined dynamic data acquired over a wide timescale facilitates the understanding, validation and modeling of the involved dynamics. In this context, fast field-cycling nuclear magnetic resonance relaxometry (FFC-NMR), in which the spin lattice relaxation time (T_1) is recorded as a function of magnetic field strength (B_o), and hence ^{1}H Larmor frequency ($\nu_o = \gamma^H B_o/2\pi$), has emerged as an optimal technique with these advantages. FFC-NMR has been successfully applied for the study of the molecular dynamics in a large number of systems, including solid polymers and polymer melts [20,21]. The dynamic information is obtained from the evolution of the net proton magnetization of the whole sample. This is strictly related to the evolution of the nuclear spins and the interactions between them, which are modulated by the molecular and mesoscopic dynamics. Several reports can be found in the literature about the use of FFC-NMR in the study the molecular dynamics in polymer melts [20,22–24], however, so far this kind of studies were not yet extended to amphiphilic copolymers in the solution state. Previous studies in polymers melts demonstrated that the ^{1}H spin-lattice relaxation is of dipolar nature, and can be explained in terms of well known established dynamic models for polymers.

1.1. Dynamics of PEO-PPO-PEO triblock copolymer micelles

While much progress has been done in the elucidation of self-assembled copolymer structures, the underlying molecular dynamics still remains poorly understood. The exchange kinetics of unimers from the bulk into the micelle and formation/breakdown of the micelles has been extensively studied over decades [17,25–34]. These two processes can be associated with different time scales, although still discrepancies persist depending on the used experimental techniques and the specimen. However, all experimental studies confirm that the faster process correspond to unimers exchange, with a characteristic time usually within a range froma few microseconds to hundreds of milliseconds [1,17,33–35]. The unimers exchange is a complex process where the hydrophobic globule of the copolymer uncoils to penetrate into the micelle's core. At expulsion, once the unimer reaches full contact with the solvent, the free copolymer tightly coils again in order to prevent the contact between the solvent and the PPO (hydrophobic block) core [33]. That is, the exchange of single copolymer molecules with the assembled micelle includes the folding and unfolding mechanism. The formation/breakdown process of micelles is in principle much slower, and not always observable with the mentioned experimental techniques. It is worth to mention that stopped flow and temperature jump techniques often used to study micellization kinetics are extremely perturbative: micelles are disrupted and the relaxation to the equilibrium state is monitored by light scattering or fluorescence [26,35]. Despite the coexistence of micelles and dissolved unimers, pulsed field gradient (PFG) NMR diffusion measurements revealed the existence of a single diffusivity for both components, attributed to the fact that the exchange rate of unimers is faster than the diffusion time scale [36].

Neutron scattering studies in undeuteratedF68 ($EO_{141}PO_{44}EO_{141}$)in D_2O and F68 with deuterated PEO blocks, revealed that a slower relaxation corresponds to Rouse modes of the PPO segments, while a faster relaxation was identified with the higher mobility of the PEO corona [37]. This faster relaxation time was found to be consistent with longitudinal diffusive modes of the PEO blocks, considering their similitude with a brush regime(-terminally attached chain) [37–39]. The method does not allow getting information about the colloidal behavior of the micelles, but reveals details of the polymeric dynamics. In view of this clear separation of the segmental dynamics between core and corona, it was suggested that the PEO/PPO interface in the micelle effectively anchors the chains on the time scale of the experiment, despite the chain exchange that may occur in the millisecond time scale [4,17,35]. This picture is also supported from proton NMR spectroscopy studies [40,41].

2. Experimental

2.1. Sample preparation

Block copolymers were obtained from BASF Corporation under the Pluronic registered tradename and used without further purification. Specifically, these were Pluronic F68 ($EO_{80}PO_{27}EO_{80}$), F108 ($EO_{141}PO_{44}EO_{141}$), and F127 ($EO_{101}PO_{56}EO_{101}$), where the numbers indicate the monomers composition and, EO and PO stand for ethylene oxide (C_2H_4O) and propylene oxide (C_3H_6O) respectively. Aqueous Pluronic solutions were prepared by dissolving at room temperature the copolymer in D_2O at the corresponding polymer weight-to-solution volume ratios. That is, the concentration of the polymer in the sample was expressed as amount of polymer weight (kg) in volume of solution (m^3). The equivalent unit of concentration in the international system of units (SI) is mol/m^3which relates to kg/m^3 as follows: mol/m^3 = (kg/m^3) x (1000/molar mass), where the molar mass is expressed in g/mol and depends on the polymer. The mixture was stored at4 to 6 °C (the equivalent unit in the SI is Kelvin K which relates to Celsius degrees as follows: K = °C + 273.15) for 12–24 h, until a homogeneous transparent solution was obtained. Then the sample was kept a few hours at the required temperature to allow (or not) micelles formation,

according to the corresponding CMT value and polymer concentration. The average sizes of the unimers and/or aggregates were determined using a Nicomp 380 High Performance Particle Sizer (HPPS).

2.2. Nuclear magnetic relaxation dispersion experiments

^{1}H spin-lattice relaxation time dispersions in the laboratory frame (T_1) were measured using the FFC-NMR technique [20,42,43] with a Spinmaster FFC-2000 Fast Field Cycling NMR Relaxometer (Stelar, Mede, Italy) for aqueous Pluronic solutions. In all cases a polarization magnetic field of 0.47 T (equivalent to 20 MHz for ^{1}H) was used, which was switched-on for a period between 1 and 2s to set-up the equilibrium magnetization (depending on the sample and the temperature). The value of the acquisition field was 0.392 T (16.7 MHz). A field slew rate of 12 MHz/ms was used in all cases, with a switching time of 2.3 ms for the account of the magnetic field level transitions. The relaxation times were determined from the magnetization recovery curves by least-squares fiting. The spin relaxation process was found to be monoexponential, within experimental error, at all frequencies for some aqueous Pluronic solutions, and biexponential for others. The sample temperature was controlled within ±1 °C using a Stelar Variable Temperature Controller. Typically, between 12 and 24 signal scans were accumulated at each delay τ (12–30 different values) and frequency (10–24 different values). Relaxation times dispersions were measured within the frequency range from 5 kHz to 20 MHz, at different concentrations (10–22.5% w/v) and temperatures (14-22 °C) for aqueous solutions of Pluronic F68, F108 and F127. These concentrations and temperatures were chosen based on the phase diagrams of these three block-copolymers, trying to get mainly unimers, micellar phase and gel phase when it was possible. Typical phase diagrams given by plots of temperature versus concentration for these block-copolymers can be easily found in literature [1,5,44].

It is worth mentioning that the polymers were dispersed in D_2O and not in H_2O to let our experiments focus on the signal coming from the protons belonging to the polymer. As a consequence, there might be protons eventually in HDO molecules formed during the sample preparation. However, the contribution to the relaxation rate due to free molecules of HDO, as they belong to the bulk water, is non-dispersive within the measured frequency range(constant contribution to the total relaxation profile).

Non-averaged local fields due to residual dipolar couplings were evaluated using the fixed lock-time rotating frame dispersion experiment [45]. A local field lower than 1 kHz was determined, so T_1 dispersions measured from a minimum frequency of 5 kHz should be free of undesirable local field effects.

^{1}H spin-lattice relaxation time dispersions in the rotating frame ($T_{1\rho}$) were measured, using the spin-lock sequence, with a Bruker Minispec mq-20 (20 MHz). Aqueous solutions at25ºCcomposed of Pluronic F68 at 10% w/v and F127 at 22.5% w/v were evaluated within a lock frequency range from 6 kHz to 22 kHz, with 16 repeat scans for each frequency. The sample temperature was controlled within ±1 °C using the temperature control unit of the Bruker Minispec instrument.

2.3. Modeling the relaxation time dispersions

For this task we essentially adopted the systematic approach previously discussed [46]. The methodology resembles a least squares fitting procedure, but in this case absolute differences between the model and experimental values are minimized instead. This practice reduces the computing time, while the final result is not critically dependent on this choice. In this method we averaged the absolute value of deviations between the model curve and the experimental data. We called this quantity SUM. It represents the percentage error of the model curve. The optimal model fitting to the data was obtained by automatically finding the best combination of model parameters that made SUM lower than a pre-defined value called SUM_{max} (typically 0.07). Parameter uncertainties were determined by analyzing the sensitivity of the optimal model curve to variations of each parameter. The error interval associated to each parameter corresponds to the maximum shift of the model curve within experimental errors.

2.4. NMR spectroscopy

A NMR spectrum of an aqueous solution of Pluronic F127 in D_2O at 10%w/v, at room temperature, was measured using a Bruker Avance III spectrometer operating at 300 MHz. The corresponding results can be found in the supplementary material. The end-group analysis from this spectrum confirmed the monomer ratios of PEO and PPO as specified by the manufacturer.

2.5. Atomic force microscopy (AFM)

Samples for AFM imaging were prepared by deposing a drop of aqueous Pluronic solutions on the sample holder and letting it dry overnight at room temperature. Samples were composed of Pluronic F68 and F127 originally solubilized in MilliQ water at 10%w/v. The AFM imaging was performed in air at 20 °C using a Bruker Innova® Atomic Force Microscope and analyzed with Nano Drive v8 real-time control and Nano Scope Analysis softwares. The scan sizes were of 1.5 μm × 1.5 μm for F68 and 2 μm × 2 μm for F127. The images can be found in the supplementary material.

3. Results

3.1. Proton spin-lattice relaxation time dispersions

The T_1 relaxation time dispersion curves measured in aqueous solutions of Pluronic F127 at 22.5%w/v can be observed in Fig. 2. This Figure shows the corresponding dispersions of the two observed components (one relaxing with a short time constant T_{1s} and other with a longer time constant T_{1l}) of the magnetization decay recorded at 14 °C and 20 °C. The sample is composed of a mixture of micelles and unimers in a sol phase at 14 °C, while it

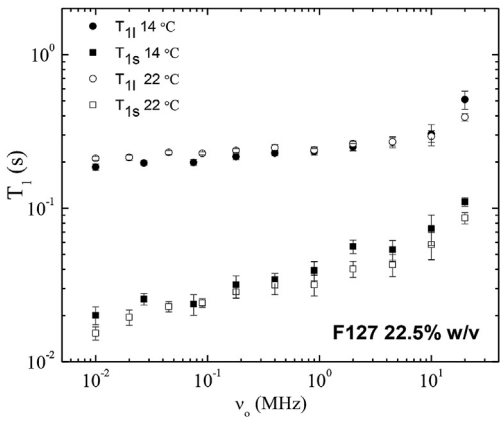

Fig. 2. Long (T_{1l}) and short (T_{1s}) dispersions of the two relaxation time components of Pluronic F127: solution at 22.5% w/v, recorded at 14 °C (filled symbols) and 22 °C (empty symbols). The sample shows a solution phase and is composed of unimers and micelles at 14 °C. It presents gel phase and is composed of micelles at 22 °C. No difference is observed between T_1 dispersions of solution and gel phases. T_{1s} seems to be more dispersive in both cases.

presents a gel phase composed of micelles at 22 °C, in agreement with the literature [5,47]. The gross phase behavior can be verified by eye due to the fact that the sample does not flow in the gel phase. The shorter T_1 shows-up with a higher dispersion. The typical bi-exponential decay of the magnetization, which was observed for all the samples of Pluronic F127, can be seen in Fig. 3 where it is clear that a mono-exponential fitting does not describe the experimental curve correctly. It is specifically shown for a solution of Pluronic F127 at 22.5% w/v recorded at 14 °C and at $B_o = 2$ MHz.

Experimental T_1 dispersions for aqueous solutions of Pluronic F68 and F108 at concentration of 22.5% w/v and recorded at 14 °C and 22 °Care shown in Figs. 4–6. For these cases, the discrimination of two exponential decays was not possible, and the magnetization decay was treated as monoexponential. According to the phase diagrams for these copolymers [1,5,48] at both measured temperatures the F68 sample corresponds to a solution phase composed of a mixture of unimers and micelles. In contrast, the F108 solution is mainly composed of unimers at 14 °C and of micelles at 22 °C. While a weak dispersion is observed at both temperatures in F68, a higher dispersion shows-up for the micellar solution of F108.

3.2. $T_{1\rho}$ profiles

$T_{1\rho}$ dispersions in the rotating frame were measured for aqueous solutions of Pluronic F68 at 10% w/v and F127 at 22.5% w/v, both cases recorded at25 °C. These profiles are shown in Fig. 7. Considering the CMT values for these polymers [1,5], the sample solution corresponds to a mixture of unimers and micelles for F68 and a micellar gel phase for F127. $T_{1\rho}$ exhibits only one component for F68, but two components are evidenced, as in the case of T_1, for F127 ($T_{1\rho s}$ and $T_{1\rho l}$). No dispersion is observed within the measured frequency range for none of them. In these figures ν_{1L} stands for the lock-frequency in the rotating frame.

4. Analysis and discussion

4.1. Pluronic F127

A bi-exponential evolution of the longitudinal magnetization $M_z(t)$ was considered for both the PP (pre-polarized) and NP (non-polarized) sequences of the magnetic field-cycling experiment [42]. Both components of T_1 show a weak dispersion, but the shorterT_{1s} is clearly more dispersive (see Fig. 2). The bi-exponential nature of

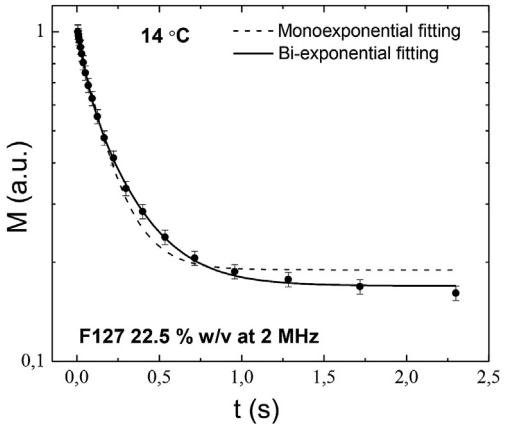

Fig. 3. Bi-exponential decay of the magnetization for a solution of Pluronic F127 at 22.5% w/v, recorded at 14 °C and at $B_o = 2$ MHz. It can be observed that a mono-exponential fitting does not describe the experimental curve correctly.

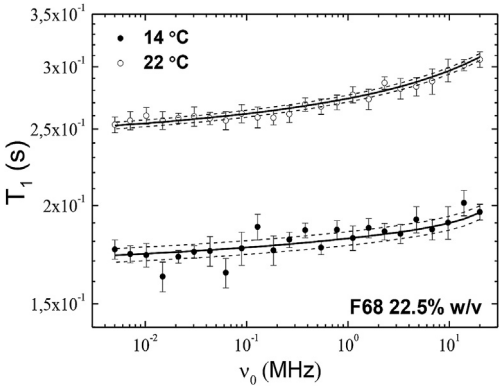

Fig. 4. T_1 dispersions of Pluronic F68 solution at 22.5% w/v, recorded at 14 °C and 22 °C. At both temperatures the sample corresponds to a solution phase composed of a mixture of unimers and micelles. A weak T_1 dispersion is observed. Model (solid black lines) corresponding to equation (6) is used to describe the experimental curves (see text for explanation).

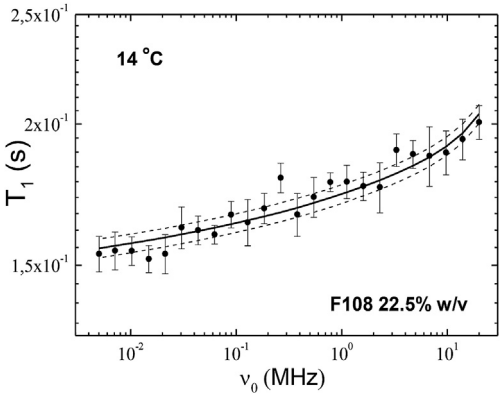

Fig. 5. T_1 dispersion of Pluronic F108 solution at 22.5% w/v, recorded at 14 °C. An unimer-dominant solution gives-up at this temperature. Model (solid black line) corresponding to equation (6) is used to describe the experimental curve (see text for explanation).

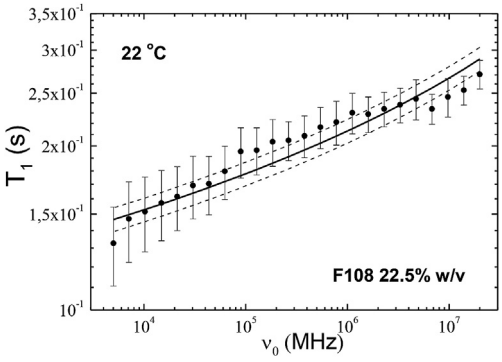

Fig. 6. T_1dispersion of Pluronic F108 solution at 22.5% w/v, recorded at 22 °C. A micelle-dominant solution gives-up at this temperature. Model (solid black line) corresponding to equation (6) is used to describe the experimental curve (see text for explanation).

T_1wasalso observed for a 10%w/v solution of F127 at 18 °C and pure Pluronic F127 in the solid phase (compacted powder without dissolving in D_2O) at 27 °C(at a proton Larmor frequency of20 MHz, using the standard inversion recovery sequence π-π/2). Moreover,

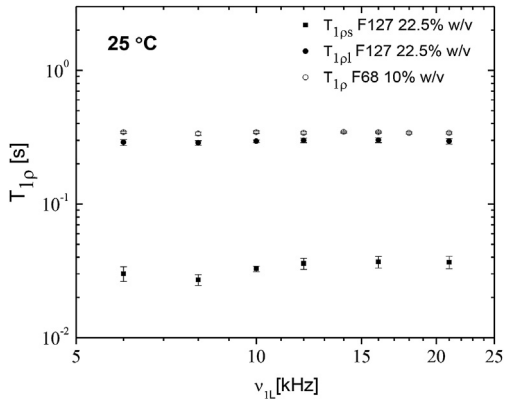

Fig. 7. $T_{1\rho}$ dispersion of Pluronic F68 solution at 10% w/v (mixture of unimers and micelles) and F127 solution at 22.5% w/v (micellar gel phase), recorded at 25 °C. No dispersion is observed in $T_{1\rho}$within the measured frequency range.

$T_{1\rho}$consistently showed two relaxation components in the rotating frame experiments (see Fig. 7). Analyzing the amplitude ratio A_j (j=s,l, long and short relaxation components amplitudes)for both the polymer in the solid phase and in solution(D_2O) at different concentrations, temperatures and frequencies, and considering that F127 contains 808 protons in the PEO block and 336 protons in the PPO block, we get:

$$R_{F127} = \frac{N°protonsPPO}{N°protonsPEO} = 0.416 =: \left[\frac{A_s}{A_l}\right]_{theoretical} \quad (1)$$

That is, the short component can be associated to the PPO block. A good agreement between the theoretical and measured ratios is observed (see Fig. 8). We can observe that the best agreement is given at lower Larmor frequencies, where the two relaxation components are better resolved.

Each component (l and s) of the T_1 dispersion profiles for F127 can be attributed to the different groups of protons belonging to the PEO and PPO blocks. This result essentially means that the experiment is independently sensitive to the dynamics of the PEO and PPO blocks and their environment (being the modulation of the dipolar interactions between the protons of each unit the probing parameter).

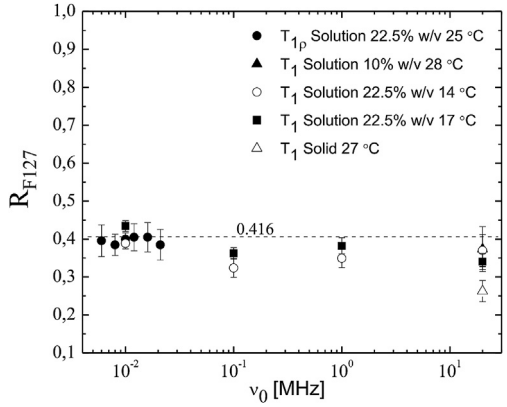

Fig. 8. Amplitudes ratio of the long and short magnetization recovery forT_1 and $T_{1\rho}$ for F127 at different concentrations, temperatures and frequencies, in the solid and solution phase. A good agreement between the theoretical and measured ratios is observed.

All the measured dispersions for F127 look similar, although it can be clearly observed that the longer T_1 components show a lower dispersion. From Fig. 1 we learn that the experiment is insensitive to the different temperatures (14 °C and 22 °C) at22.5% w/v. Although the experimental conditions of the experiments are very close to the CMC-CMT boundary, a sol phase composed of unimers and micelles corresponds to 14 °C, while a soft gel composed of micelles is obtained at 22 °C. Interestingly, the T_1-dispersions are completely insensitive to these two situations. That is, the observed dynamics is independent of the aggregation state of the copolymers.

In the dilute regime, copolymers behave as independent entities dissolved in the aqueous environment. However, from previous studies it was inferred that the unimers tend to form a PPO hydrophobic core surrounded by the hydrophilic PEO blocks, that is, monomolecular micelles [49]. This is the main reason why the unimer to micelle transition spans over a concentration or temperature decade [5], and a pre-micelle state forms close to the CMT or CMC boundary [50]. It was also suggested that in a broad temperature range above the CMT, spherical micelles coexist in solution with unimers [5]. Moreover, the lifetime of the copolymer in the micelle may be less than 3 ms, that is, a fast-exchange process occurs between the unimers and the micelles [51]. All these facts support the insensitiveness of the measured dispersions to the state of aggregation of the copolymer, and allow us to assume that, at least for F127, the observed dynamics corresponds to the triblock copolymer itself, independently of the aggregation state.

Independently of the aggregation state corresponding to the different selected temperatures, for the concentration of 22.5% w/v, our results suggest that the involved dynamics does not change drastically within the explored temperature interval. The reader should be advised that in this technique we do not have spectral resolution, and keep present that the detected signal originates in the average contribution of all the protons, as detected in a low-resolution limit. However, protons belonging to the PEO and PPO units of the copolymer can be discriminated from its relaxation behavior. The weak temperature dependence of T_1 for PEO-PPO-PEO block copolymers within the measured temperature range of our work was also observed at high-resolution NMR [40]. Both, the methylene protons in the PEO block and the methyl protons of the PPO block show a weak temperature-dependence.

In order to explain the observed dispersions, we refer to the established models obtained for homopolymers in solution and melts, respectively. The theory for the dynamics of linear homopolymers predicts two different NMR regimes depending on chain length and concentration. Below a critical molecular weight, the frequency dependence of the longitudinal relaxation time in melts is characterized by Rouse dynamics, i.e. [23]:

$$T_1^{-1}(\omega) \propto -\tau_s \ln(\omega\tau_s) \quad \text{for } \tau R^{-1} << \omega << \tau s^{-1} \quad (2)$$

$$T_1^{-1}(\omega) \propto \tau_s ln\,(N) \text{ for } \omega << \tau \mathrm{R}^{-1} \quad (3)$$

where τ_s and τ_R are the segmental relaxation time and the Rouse time, respectively, i.e. the relaxation time of the longest Rouse mode of the chain consisting of N Kuhn segments, with $\tau_R = \tau_s N^2$. Above the critical molecular weight W_c, entanglements set in and the T_1 dispersion changes towards power-laws with different exponents in different frequency regimes [20]. The value of W_c has been estimated as 5800 g/mol for PEO [52] and 7000 g/mol for PPO [53], respectively. Apart from polymer melts with short chains for which $W < W_c$, Rouse behaviour is also observed in polymer solutions with concentrations below the onset of physical entanglements(very diluted solution). Although the total molecular weights

of all three Pluronic samples are above the critical weight for both homopolymers (about 12200 g/mol for F127, 8700 g/mol for F68 and 15000 g/mol for F108), these polymers are studied in solutions at concentrations where entanglements do not play a role in the polymer dynamics and therefore it is expected they feature Rouse behaviour. In particular, the solvated state of the copolymer may favour this behaviour.

For Θ diluted solutions, where the polymeric chains are considered as ideal chains, the Zimm model applies [54]. While the essential assumption of the Rouse model is that the dynamics is governed by the interactions localized along the chain, for the Zimm model, the interactions along the segments are not localized [55]. Strictly speaking, a Θ dilution cannot be associated neither to the hydrophilic PEO block nor to the hydrophobic PPO block. However, when copolymers are arranged in micelles, and assuming that entanglement is prevented by the presence of hydration within the core of the micelle, the Rouse model can be used to explain the observed dispersion. A similar approach holds for the entanglement-free monomolecular structure.

Indeed, the frequency dependence of the short component of T_1(PPO) in F127can be fitted by the Rouse equation(equation (2)) [23]:

$$T_{1s}(\nu) = \left[C_{Rs}\tau_{ss}\, ln\left(\frac{1}{2\pi\,\nu\,\tau_{ss}}\right)\right]^{-1} + C_s \qquad (4)$$

where C_{Rs} is a constant that depends on the proton magnetogyric ratio γ and on the mean interproton distance; C_s is an offset constant, and the τ_{ss} corresponds to the segmental relaxation time associated to the short T_1 component. From this result, it turns out that the Rouse dynamics can fully explain the observed dispersions for the PPO block of F127 at both concentrations and temperatures as shown in Figs. 9–11. Moreover, within the measured frequency range, the Rouse dynamics is dominant over the fast internal motions of the chain. It can be argued that for both micelles and unimers, the local cooperative segmental dynamics is purely governed by the PPO chain properties, in full agreement with previous studies using high-resolution proton NMR [40]. A segmental correlation time of the order of10^{-9}s was obtained for all the three cases as it is presented in Table 1, in agreement with the frequency limits established in equations (2) and (3).

It is reasonable to assume that the Rouse dynamics is also present in the PEO blocks. Comparing the involved physical parameters, the segmental correlation time of both blocks is expected to be of the same order. However, PEO blocks may show *trans*-defects in the chains that tend to stabilize into gauche conformers as the temperature is increased, show in general a higher degree of hydration, and a higher disordered state [56]. The picture of *trans*-gauche fluctuations, a higher interaction with the surrounding water and a more disordered state, plays in favour of a higher mobility of the PEO blocks. In addition, we may consider longitudinal diffusive processes that may be effective in a brush regime [39]. This fact is consistent with the lower dispersion observed in the long component of T_1 (see Figs. 2 and 9). On these grounds, we explain the observed dispersions by considering a Rouse term plus a Lorentzian term for the account of these extra-processes affecting the PEO blocks, not observed in the short component of T_1. In spite of the fact that a Rouse term alone can also describe the dispersion in this case, an inconsistency related to the values of the segmental times as a function of the polymer molecular weight is obtained. More details about this will be given later in the manuscript. Therefore, the long component of the spin-lattice relaxation time can be described by:

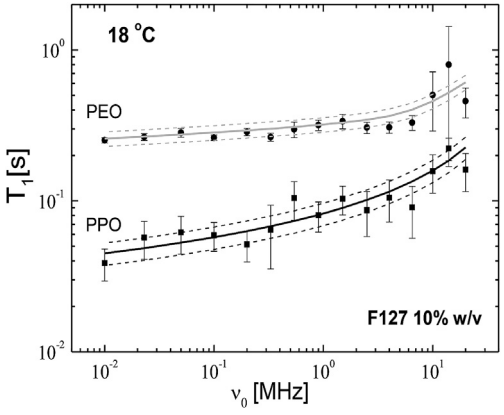

Fig. 9. Long (T_{1l}) and short (T_{1s}) dispersions of the two relaxation time components of Pluronic F127 solution at 10% w/v, recorded at 18 °C. T_{1s} shows up a higher dispersion. The sample is composed of unimers and micelles. Models (solid lines) corresponding to equation (4) (black line) and (5) (light grey line) are used to describe the experimental curves (see text for explanation).

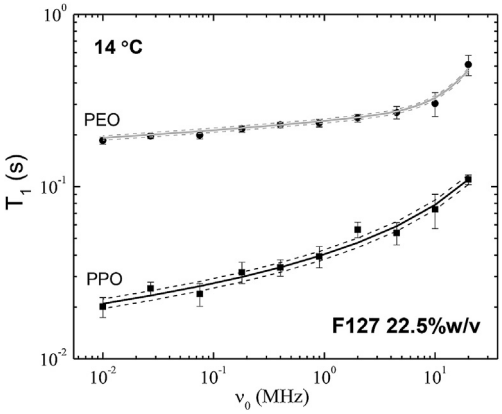

Fig. 10. Long (T_{1l}) and short (T_{1s}) dispersions of the two relaxation time components of Pluronic F127solution at 22.5% w/v, recorded at 14 °C. The sample shows a solution phase and is composed of unimers and micelles. Models (solid lines) corresponding to equation (4) (black line) and (5) (light grey line) are used to describe the experimental curves (see text for explanation).

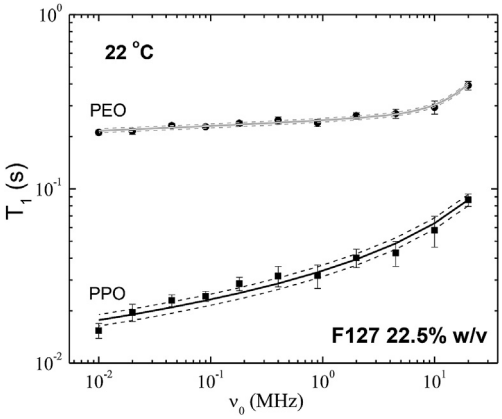

Fig. 11. Long (T_{1l}) and short (T_{1s}) dispersions of the two relaxation time components of Pluronic F127solution at 22.5% w/v, recorded at 22 °C. Models (solid lines) corresponding to equation (4) (black line) and (5) (light grey line) are used to describe the experimental curves (see text for explanation).

$$T_{1l}(\nu) = \left[C_L \left(\frac{\tau_L}{1 + (2\pi\,\nu\,\tau_L)^2} + \frac{4\,\tau_L}{1 + (4\pi\,\nu\,\tau_L)^2} \right) + C_{Rl}\,\tau_{sl}\,ln\left(\frac{1}{2\pi\,\nu\,\tau_{sl}}\right) \right]^{-1} + C_l, \tag{5}$$

where τ_L is correlation time of the Lorentzian term which represents a temperature dependent characteristic time (it depends on the temperature according to an Arrhenius law) associated with the extra-processes affecting the PEO blocks, C_L the corresponding amplitude and C_l is again an offset constant.

The resulting curves are presented in Figs. 9–11, and the corresponding parameters in Table 1. A good agreement between the model of equation (5) and the experimental curves is observed.

A segmental correlation time of the order of 10^{-10}s was obtained for the long component of T_1 for the three analyzed cases, as it is presented in Table 1. It can be observed that τ_{ss} is larger than τ_{sl} for all samples and both of them tend to decrease slightly when the temperature increases at 22.5%w/v concentration, in agreement with literature [57,58].

On the other hand, τ_L does not show significant variations with temperature change but it becomes shorter with increasing polymer concentration (see Table 1). Correlation times of the order of 0.27ns were attributed to chain backbone rearrangements in polystyrene in C_6D_6 from ^{19}F and ^{13}CNMR spectroscopy [59,60]. The dynamics of deuterated PEO-d_4 in aqueous solution at different concentrations was studied using standard magnetic field-dependent ^2H relaxation experiments [61]. In concentrated solutions, results were interpreted in terms of three Lorentzian spectral densities, for the account of "slow", "medium" and "fast" motions. A high internal mobility of the PEO chains turns consistent with the interpretation of our data, even at high concentrations where cross-linking is feasible, as revealed by the flat dispersions of the relaxation time. Correlations times in the range 1.4–4.8ns were found for the account of "medium" processes, tentatively attributed to partially hindered reorientations of a dynamic unit (considered to be of the order of a Kuhn segment). At low concentrations, the observed dynamics becomes independent of W, indicating local length scale reorientations. In this limit, correlation times of the order of 1.3–1.6ns were interpreted in terms of isotropic overall rotations of the Kuhn segment.

4.2. F68 and F108

Our analysis of the proton spin-lattice relaxation time dispersions for F127 reveals the existence of independent dynamical processes for PPO and PEO blocks. However, this result cannot be directly translated to F68 and F108 since the bi-exponential decay is not observed in these cases. The mono-exponential decay can be explained by the proton ratio R between the PPO and PEO units for the copolymers F68 and F108 using equation (1). They are $R_{F68} = 0.253$ and $R_{F108} = 0.234$, which are considerably smaller than R_{F127}=0.416. This means that the amount of protons in the PPO and PEO blocks are more similar to each other for F127 in comparison to F68 and F108. In other words, the bi-exponential relaxation in F68 and F108 is most probably partially masked by the relative quantity of protons of each block that contributes to the NMR signal, and may also happen that the short and long components get closer. However, it turns out that against this experimental indecisiveness, one can assume at a low risk that the main relaxation mechanisms that are effective in F127 are essentially the same for F68 and F108. That is, despite the fact that the used technique cannot distinguish the two relaxation components corresponding to each block, we may assume that the same dynamical model applies in all cases. Then, we check for the consistency with the measured dispersions.

A unique Rouse function for the whole polymer may be questionable, since there is a density modulation along the chain that may violate the theoretical conditions of the model. Therefore, we propose to preserve the previous model (equation (4) and (5)), now considering the fact that the contribution of all the protons is included in the measured dispersion. That is, we consider the superposition of a Rouse term for the account of the PPO dynamics, and a Rouse plus a Lorentzian term for the account of the PEO dynamics. These contributions are to be weighted by the corresponding relative proton density of each block:

$$T_1(\nu) = \left[A_{PEO} \left(C_L \left(\frac{\tau_L}{1 + (2\pi\,\nu\,\tau_L)^2} + \frac{4\,\tau_L}{1 + (4\pi\,\nu\,\tau_L)^2} \right) + C_{Rl}\,\tau_{sl}\,ln\left(\frac{1}{2\pi\nu\tau_{sl}}\right) \right) + A_{PPO} \left(C_{Rs}\,\tau_{ss}\,ln\left(\frac{1}{2\pi\,\nu\,\tau_{ss}}\right) \right) \right]^{-1} + C \tag{6}$$

where the amplitudes A_{PEO} and A_{PPO} represent the relative contribution of each block to the total population of protons. Considering that their sum is equal to unity and that

$$\left(\frac{A_{PPO}}{A_{PEO}}\right)_{F68} = 0.253 \left(\frac{A_{PPO}}{A_{PEO}}\right)_{F108} = 0.234 \tag{7}$$

we obtained for F68 that $A_{PEO} = 0.798$ and $A_{PPO} = 0.202$, and for F108 $A_{PEO} = 0.810$ and $A_{PPO} = 0.190$.

It is worth mentioning that equation (6) considers two distinct values of the time τ_s for the PEO and PPO blocks, namely τ_{sl} and τ_{ss} respectively. In order to estimate their values, we use a model proposed by other authors for segmental relaxation time (α-relaxation in dielectric relaxation experiments) as a function of polymer molecular weight W [62]:

$$\tau_s(W) = \frac{\tau_s(\infty)}{1 + (W_{lim}/W)^2} \tag{8}$$

The value corresponding to the ideal chain of infinite length $\tau_s(\infty)$, is obtained already for molecular masses above W_{lim}, a limiting molecular weight for the dependence of τ_s on W (usually around 10.000). The α-relaxation time has been discussed in other works [62,63] where the authors attribute a similarity between segmental α-relaxation in dielectric relaxation experiments, and the Rouse segmental relaxation. The main reason for this

Table 1
Parameters obtained from the fittings using models given by equations (4) and (5) for the measured spin-lattice relaxation time profiles of Pluronic F127, at different concentrations and temperatures.

Parameters		Sample		
		F127 10%w/v(18 ± 1)ºC	F127 22.5%w/v(14 ± 1)ºC	F127 22.5%w/v (22 ± 1)ºC
T_{1s}	τ_{ss} [s] $\times 10^{-10}$	17 ± 3	15 ± 3	12 ± 2
PO segment	C_{Rs} [s^{-2}] x10^9	1.8 ± 0.3	3.7 ± 0.3	5.2 ± 0.3
	C_s [s]	0.008 ± 0.006	0.001 ± 0.001	0.0003 ± 0.0003
T_{1l}	τ_{sl} [s] $\times 10^{-10}$	2.8 ± 0.6	7.4 ± 0.9	5.7 ± 0.7
	C_{Rl} [s^{-2}] x10^9	1.6 ± 0.3	0.47 ± 0.06	0.71 ± 0.09
PEO segments	τ_L [s] $\times 10^{-9}$	8 ± 3	4.8 ± 0.4	4.5 ± 0.3
	C_L[s^{-2}] x10^8	0.5 ± 0.2	1.3 ± 0.1	2.0 ± 0.2
	C_l [s]	0.12 ± 0.02	0.040 ± 0.007	0.10 ± 0.05

Table 2
Parameters obtained from the fittings using models given by equation (6) for experimental spin-lattice relaxation time profiles of Pluronic F68 and F108 at 22.5%w/v and different temperatures.

Parameters		Sample			
		F68 22.5%w/v (14 ± 1)ºC	F68, 22.5%w/v(22 ± 1)ºC	F108, 22.5%w/v(14 ± 1)ºC	F108, 22.5%w/v (22 ± 1)ºC
PPO segment	τ_{ss}x10^{-10}[s]	3.0 ± 0.6	2.4 ± 0.5	8 ± 2	6 ± 1
	C_{Rs}x10^9[s^{-2}]	1.0 ± 0.1	5.1 ± 0.6	1.5 ± 0.2	0.7 ± 0.1
PEO segments	τ_{sl}x10^{-10}[s]	6 ± 1	4.2 ± 0.8	14 ± 3	11 ± 2
	C_{Rl}x10^9[s^{-2}]	9 ± 1	8 ± 1	1.7 ± 0.3	0.38 ± 0.07
	τ_Lx10^{-9}[s]	1.8 ± 0.4	0.37 ± 0.07	1.6 ± 0.3	0.26 ± 0.08
	A_L x10^8[s^{-2}]	24 ± 6	23 ± 6	15 ± 3	25 ± 8
	C [s]	0.16 ± 0.03	0.22 ± 0.06	0.12 ± 0.03	0.005 ± 0.002

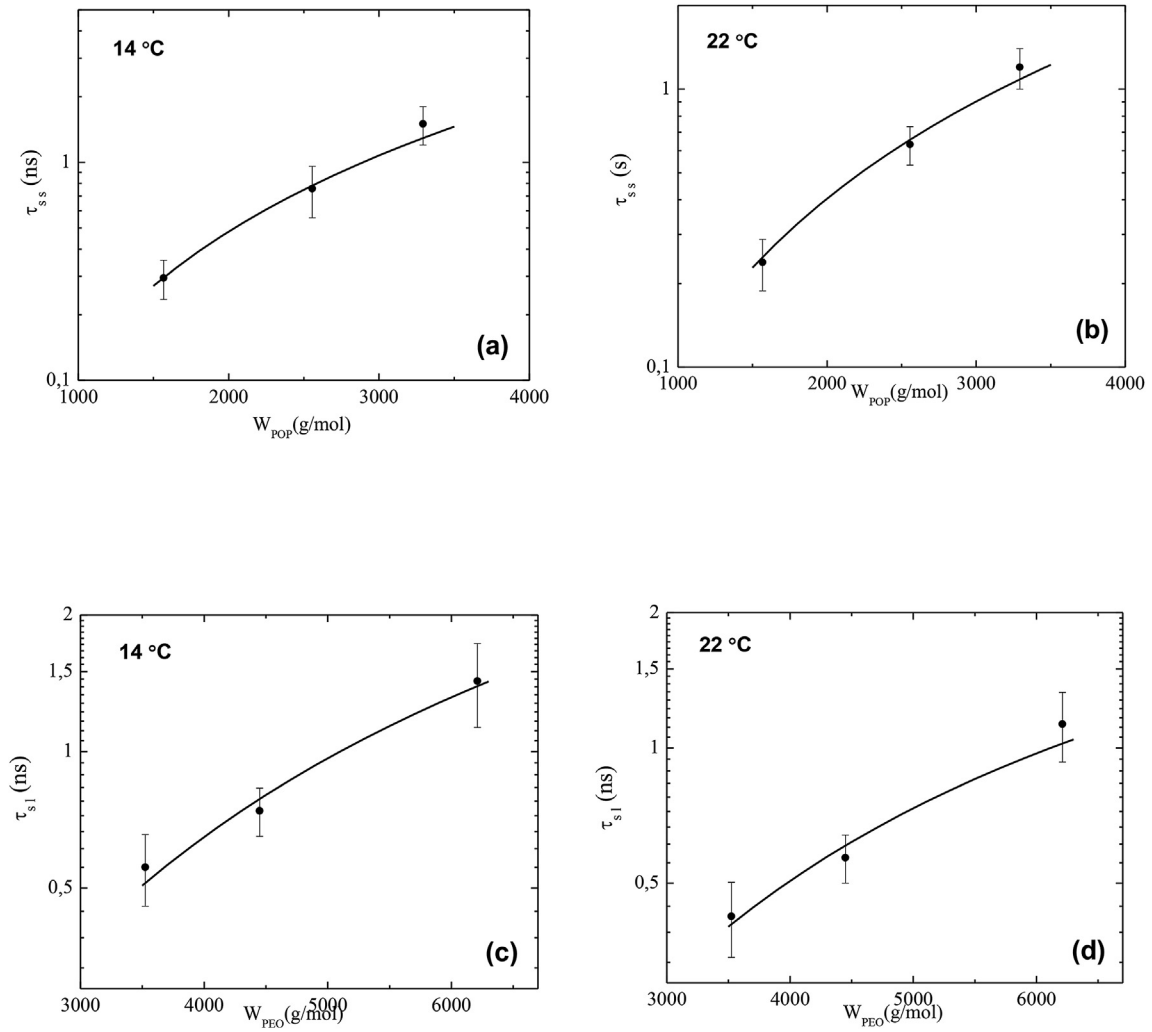

Fig. 12. The values of τ_{ss} and τ_{sl} as a function of molecular weight of the block at different temperatures are described by the model of equation (8). a) PPO 14 °C, b) PPO 22 °C, c) PEO 14 °C and d) PEO 22 °C.

Table 3
Parameters for the curves given by equation (8) that describe the segmental times as a function of polymer molecular weight, at different temperatures.

Parameters	PPO at 14 °C	PPO at 22 °C	PEO at 14 °C	PEO at 22 °C
$\tau_s(\infty)$[s]	$(9 \pm 1) \times 10^{-8}$	$(8 \pm 1) \times 10^{-8}$	$(7.5 \pm 0.8) \times 10^{-9}$	$(3.7 \pm 0.6) \times 10^{-9}$
W_{lim} [g/mol]	28000 ± 3000	27000 ± 2000	13000 ± 1000	10000 ± 1000

comparability is the fact that they are found in the same order of magnitude, which has been established for a wide range of polymers and it is 10^{-10}-10^{-8}s in a temperature range around 17-27 °C [57,58]. In addition, it is worth to mention that equation (8) a molecular weight W dependence of τ_s that is consistent with the Rouse model [64].

The values of τ_{ss} and τ_{sl} for F68 and F108 were estimated using the following procedure:

(i) Calculate $\tau_s(\infty)$ and $W_{lim}$by considering that τ_{ss} and τ_{sl} obtained through equations (4) and (5)for F127 (see Table 1) follow the model of equation (8).
(ii) Estimate the potential ranges for τ_{ss} and τ_{sl} for F68 and F108 by introducing the parameters already calculated in the previous step and their corresponding molecular weights for PPO and PEO blocks into equation (8).
(iii) Use equation (6) to fit the T_1 profiles of F68 and F108, where τ_{ss} and τ_{sl} values are within the ranges determined in step (ii).

The optimal model curves are presented in Fig. 4 for F68 and in Figs. 5 and 6 for F108. The corresponding parameters are presented in Table 2. A good agreement between the model of equation (6) and the experimental curves is observed. Both segmental times tend to decrease when temperature increases in agreement with literature [57,58]. On the other hand, τ_L shows a significant decrease with growing temperature (see Table 2).

As shown in Fig. 12, the values of τ_{ss} and τ_{sl} as a function of the polymer molecular weight are described by the model of equation (8) very well. The corresponding parameters are shown in Table 3. It can be observed that τ_{ss} and τ_{sl} depend strongly on the molecular weight of PPO and PEO respectively. The segmental dynamics becomes slower with increasing molecular weight in agreement with literature [62,65]. It is interesting to note that both $\tau_s(\infty)$ and W_{lim} depend on temperature and specimen as shown in Table 3.

As previously mentioned, T_{1I} dispersion of F127 can be described by using only a Rouse model. However, the relaxation profiles of F68 and F108 cannot be fitted precisely without considering the Lorentzian term. This is shown exemplary in Fig. 13 for F108 solution at 22.5%w/v recorded at 14 °C. On the other hand, if these imprecise fittings are considered, the values of the segmental time do not fulfill the expected tendency as a function of molecular weight given by equation (8). For these two reasons we considered that is mathematically and physically correct to consider the models given by equations (4)–(6) to describe the relaxation profiles for the three block-copolymers.

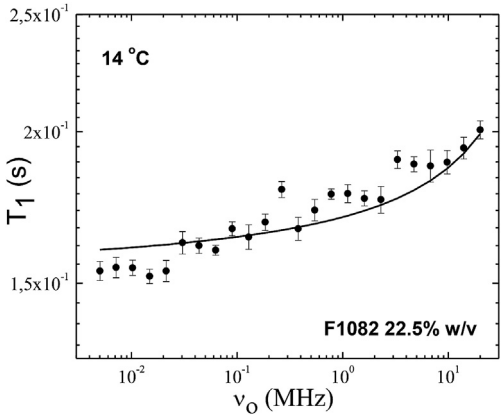

Fig. 13. T_1 dispersion of Pluronic F108 solution at 22.5% w/v, recorded at 14 °C. Model (solid line) corresponding to equation (6) without the Lorentzian term is used to describe the experimental curve (see text for explanation). It can be clearly seen that the experimental curve cannot be correctly described by the model curve if the Lorentzian term is not considered (compare with Fig. 5).

A common observation that can be made based on the discussed data is the fact that the presence of micelles does not affect the polymer motion in a qualitative manner, an assumption which is supported by the notion that molecules are not fixed in micelles but are in permanent exchange with their environment. Micelles thus do not significantly restrict the molecular mobility, and their dynamics is qualitatively equivalent to the unimer case, where isolated molecules are moving in a solvent environment. Nevertheless, the central PPO blocks appear to be less mobile than the outlying PEO blocks. Since even the total length of the molecules is just barely above the critical molecular weight for melts, the diluting effect of only a small amount of solvent – as it is present in the micelles where its concentration is lower than outside the micelles – appears sufficient to prevent entanglements to happen. This concept can be tested by comparison with Pluronic of even longer chain lengths where eventually a crossover to reptation-like dynamics, correlated with power-law relations of $T_1(\nu)$, is expected.

5. Conclusions

In this manuscript we have shown for the first time that proton NMR relaxometry can be considered as a potential experimental technique for the study and characterization of the molecular dynamics in block copolymers for the example of the commercial product Pluronics. In particular, when the proton density of the PEO and PPO blocks are not too dissimilar, the technique allows a discrimination of the associated dynamics of each block.

This fact opens up the possibility to analyze a more complex situation where the polymeric micelles become aditivated with specific drugs, through a localized sensitivity on the dynamical effects caused independently on the PEO and PPO blocks. A further research with this motivation turns essential: how can the system be stable as a drug carrier in the presence of a fast exchange of monomers entering and exiting the micelle?

Measured dispersions could be successfully explained using the Rouse model. This requires some conditions that are in a limiting situation according to the molecular weight of the analyzed specimens. However, the solvent dilution seems to be an efficient mechanism to prevent entanglement. It should be interesting to analyze the case of Pluronics of higher molecular weights: is there a limit where entanglement would be observable using NMR relaxometry through a typical power law?

A further study with Pluronics of higher molecular weights and including additivation should be considered for a better understanding of the potentialities of field-cycling NMR relaxometry for the characterization of block copolymers in solutions.

Acknowledgements

The authors acknowledge financial support from a bilateral project BMBF-Mincyt, Foncyt PICT 2013-1380 (Argentina) and ARG 11/032 01DN12087 (Germany). EA also acknowledges Alexander von Humboldt Foundation for the support during this project. AFM images were obtained at CEMETRO, Universidad Tecnológica Nacional by Dr. Daniel Brusa (Córdoba - Argentina). The authors also acknowledge to A. Sosnik and R. Glisoni from Faculty of Pharmacy and Biochemistry, Universidad Nacional de Buenos Aires (Argentina) for advising on sample preparation and for providing the Pluronic specimens.

Appendix A. Supplementary data

Supplementary data related to this article can be found at https://doi.org/10.1016/j.polymer.2018.07.027.

References

[1] P. Alexandridis, J.F. Holzwarth, T.A. Hatton, Macromolecules 27 (1994) 2414.
[2] I.W. Hamley, Block Copolymers in Solution: Fundamentals and Applications, Wiley, West Sussex, 2005.
[3] G. Riess, Prog. Polym. Sci. 28 (2003) 1107.
[4] G.F. Gohy, Adv. Polym. Sci. 190 (2005) 65.
[5] P. Alexandridis, T.A. Hatton, Colloids surf, A Physicochem. Eng. Asp. 96 (1995) 1.
[6] K. Hyun, J.G. Nam, M. Wilhellm, K.H. Ahn, S. Jong Lee, Rheol. Acta 45 (2006) 239.
[7] G. Wanka, H. Hoffmann, W. Ulbricht, Macromolecules 27 (1994) 4145.
[8] W. Brown, K. Schillen, M. Almgren, S. Hvidt, P. Bahadur, J. Phys. Chem. 95 (1991) 1850.
[9] P. Sen, S. Ghosh, K. Sahu, S. Kumar Mondal, D. Roy, K. Bhattacharyya, J. Chem. Phys. 124 (2006) 204905.
[10] Y. Rharbi, Macromolecules 45 (2012) 9823.
[11] K. Prochazka, D. Kiserow, C. Ramireddy, Z. Tuzar, P. Munk, S.E. Webbe, Macromolecules 25 (1992) 454.
[12] M. de Pooter, P.B. Smith, K.K. Dohrer, K.F. Bennet, M.D. Meadows, C.G. Smith, H.P. Schouwenaars, R.A. Geerards, J. Appl. Polym. Sci. 42 (1991) 399.
[13] J. Ma, C. Guo, Y. Tang, J. Wang, L. Zheng, X. Liang, S. Chen, H. Liu, J. Colloid Interface Sci. 299 (2006) 953.
[14] H. Tanaka, T. Nishi, Phys. Rev. B 33 (1986) 32.
[15] G. Fleischer, J. Chem. Phys. 97 (1993) 517.
[16] F. Cau, S. Lacelle, Macromolecules 29 (1996) 170.
[17] E. Hecht, H. Hoffmann, Colloids surf, A Physicochem. Eng. Asp. 96 (1995) 181.
[18] G. Waton, B. Michels, R. Zana, J. Colloid Interface Sci. 212 (1999) 593.
[19] K. Mortensen, J. Phys. Condens. Matter (1996) 8. A103.
[20] R. Kimmich, E. Anoardo, Progr. NMR Spectrosc 44 (2004) 257.
[21] R, Kimmich, N. Fatkullin, Progr. NMR Spectrosc 101 (2017) 18.
[22] R. Kimmich, Bull. Magn. Reson. 1 (1980) 195.
[23] R. Kimmich, N. Fatkullin, Adv. Polim. Sci. 170 (2004) 1.
[24] D. Kruk, H. Herrmann, E.A. Rössler, Prog. NMR spectrosc. 63 (2012) 33.
[25] E.A.G. Aniansson, S.N. Wall, J. Phys. Chem. 78 (1974) 1024.
[26] A. Halperin, S. Alexander, Macromolecules 22 (1989) 2403.
[27] T. Haliloglu, I. Bahar, B. Erman, W.L. Mattice, Macromolecules 29 (1996) 4764.
[28] E. Dormidontova, Macromolecules 32 (1999) 7630.
[29] Y. Rharbi, M. Li, M.A. Winnik, K.G. Hahn, J. Am. Chem. Soc. 122 (2000) 6242.
[30] Y. Rharbi, M.A. Winnik, Adv. Colloid Interface Sci. 89–90 (2001) 25.
[31] T. Thurn, S. Couderc-Azouani, D.M. Bloor, J.F. Holzwarth, E. Wyn-Jones, Langmuir 19 (2003) 4363.
[32] Y. Rharbi, N. Bechthold, K. Landfester, A. Salzman, M.A. Winnik, Langmuir 19 (2003) 10.
[33] R. Zana, C. Marques, A. Johner, Adv. Colloid Interface Sci. 123–126 (2006) 345.
[34] G.A. Denkova, E. Mendes, M.-O. Coppens, Soft Matter 6 (2010) 2351.
[35] I. Goldmints. Ph.D thesis, MIT, Cambridge, 1997.
[36] K. Ulrich, P. Galvosas, J. Karger, F. Grinberg, Materials 5 (2012) 966.
[37] H. Yardimci, B. Chunga, J.L. Hardenm, R.L. Leheny, J. Chem. Phys. 123 (2005) 244908.
[38] G.E. Yakubov, B. Loppinet, H. Zang, J. Rühe, R. Siegel, G. Frytas, Phys. Rev. Lett. 92 (2004) 115501.
[39] P.G. De Gennes, J. Colloid Interface Sci. 27 (1987) 189.
[40] F. Cau, F. Lacelle, Macromolecules 29 (1996) 170.
[41] J. Ma, C. Guo, Y. Tang, J. Xiang, S. Chen, J. Wang, H. Liu, J. Colloid Interface Sci. 312 (2007) 390.
[42] E. Anoardo, G. Galli, G. Ferrante, Appl. Magn. Reson. 20 (2001) 365.
[43] G. Ferrante, S. Sykora, Adv. Inorg. Chem. 57 (2004) 405.
[44] S. Jeon, S. Granick, K.-W. kwan- Kwon, K. Char, J. Polym. Sci. B Polym. Phys. 40 (2002) 2883.
[45] J. Perlo, E. Anoardo, J. Magn. Reson. 181 (2006) 262.
[46] C.C. Fraenza, E. Anoardo, Biophys. Chem. 228 (2017) 38.
[47] S.Y. Lee, Y. Lee, J.E. Kim, T.G. Park, C.-H. Ahn, J. Math. Chem. 19 (2009) 8198.
[48] P. Alexandridis, T. Nivaggioli, T.A. Hatton, Langmuir 11 (1995) 1468.
[49] K.N. Prasad, T.T. Luong, A.T. Florence Joel Paris, C. Vaution, M. Seiller, F. Puisieux, J. Colloid Interface Sci. 69 (1979) 225.
[50] L. Jia, C. Guo, L. Yang, J. Xiang, Y. Tang, C. Liu, H. Liu, J. Colloid Interface Sci. 345 (2010) 332.
[51] G. Fleisher, J. Phys. Chem. 97 (1993) 517.
[52] R.P. Wool, Macromolecules 26 (1993) 1564.
[53] B.A. Smith, E.T. Samulski, L.-P. Yu, M.A. Winnik, Macromolecules 18 (1985) 1901.
[54] B.H. Zimm, J. Chem. Phys. 24 (1956) 269.
[55] M. Doi, S.F. Edwards, The theory of polymer dynamics, International Series of Monographs on Physics 73, Clarendon Press–Oxford (1986).
[56] C. Guo, H.Z. Liu, J.Y. Chen, Colloid Polym. Sci. 277 (1999) 376.
[57] J. Mijovic, M. Sun, Y. Han, Macromolecules 35 (2002) 6417.
[58] J. Zhao, L. Zhang, M.D. Ediger, Macromolecules 41 (2008) 8030.
[59] J. Schaefer, D.F.S. Natusch, Macromolecules 5 (1972) 416.
[60] K. Matsuo, K.F. Kuhlman, W.-H. Yang, F. Geny, W.H. Stockmayer, A.A. Jones, J. Polym. Phys. 15 (1977) 1347.
[61] T.W.N. Bieze, J.R.C. van der Maarel, C.D. Eisenbach, J.C. Leyte, Macromolecules 27 (1994) 1355.
[62] C. Riedel, A. Alegría, P. Tordjeman, J. Colmenero, Macromolecules 42 (2009) 8492.
[63] Y.H. Lin, J. Phys. Chem. B 109 (2005) 17670.
[64] M. Doi, S.F. Edwards, The Theory of Polymer Dynamics, Clarendon Press, Oxford, 1998, pp. 91–94.
[65] Y. He, T.R. Lutz, M.D. Ediger, C. Ayyagari, D. Bedrov, G.D. Smith, Macromolecules 37 (2004) 5032.